Field dynamic balancing for AMBs supporting rotor shaft based on extended state observer

Kexiang Li*, Zhiquan Deng**, Cong Peng, Jiaxi He

College of Automation Engineering, Nanjing University of Aeronautics and Astronautics, China
*E-mail: lkxzdh@nuaa.edu.cn, **E-mail: dzq@nuaa.edu.cn

***Abstract* — There are promising applications for high rotational speed machines supported by active magnetic bearings (AMB), whereas it is inevitable that the rotor shafts own unbalance masses more or less. Field dynamic balancing based on disturbance observer was proposed, which could effectively eliminate vibrations derived from unbalances. A band-pass filter was cascaded after the observer, which could weaken the effects from harmonic or noise disturbances. Frequency responses were measured to compensate the characteristics of the observation module to enhance the accuracy. With the precise identification results, rotor dynamic balancing could be carried out to revise the unbalances, which was verified by simulation results.**

I. INTRODUCTION

Mass unbalance problem of rotor shaft is inevitable for rotating machineries, which could bring about vibrations. As for suspended rotor shaft supported by active magnetic bearings (AMB), vibration problems derived from mass unbalance exist as well. The machinery will vibrate significantly when rotating around the resonance speed, and it will simultaneously bring about increasing suspension power consumption and lower suspended accuracy.

Field dynamic balancing is a good way to calculate the rotor shaft unbalance in operation and then correct it on balancing discs, of which the big difference from mechanical dynamic balancing is without need to disassemble the machine. With this technique, the rotor's inertia axis would be aligned with its geometric axis, and the displacement fluctuations and vibrations could be eliminated simultaneously in operation[1].

For rigid rotor shaft, many field dynamic balancing methods have been studied based on different algorithems. One is to use displacement signals and the other is current signals. Influence coefficient method based on displacement information was put forward first. The principle of this method is similar to that of mechanical dynamic balancing, that influence coefficient can be derived through trial weighting, and then unbalance information will be calculated easily[2, 3]. Nevertheless, different from rotor shaft supported by mechanical bearings, the displacement sensor runout and some noises can also result in other vibrations in rotor-AMB systems. One solution to this problem is to introduce relative influence coefficient method to eliminate multi-frequency harmonic disturbs[4]. Kai, Z et al. [5] introduced general notch filter to identify unbalance distribution, which was also an effective way to enhance the accuracy.

This work was supported by Funding of Jiangsu Innovation Program for Graduate Education (KYLX16_0359) and Fundamental Research Funds for the Central Universities.

With the development of zero-displacement or zero-force control algorithms, some scholars adopted these methods to realize field dynamic balancing. Based on zero-force control, displacement signals could be adopted to calculate the unbalance information, which can be found in [6, 7]. Xiangbo, X et al. [6] also took multi-frequency harmonic disturb effects into consideration to realize well imbalance compensation. The other algorithm called zero-displacement method was adopted to calculate the unbalance information [1, 8]. They supposed that the resultant force of suspension forces was equal to that of centrifugal forces and the couple of the suspension forces was equal to that of centrifugal forces as well, when rotor shaft was operating with zero-displacement method. As a result, the equivalent vector of correction could be calculated by current information.

As mentioned above, the influence coefficient method needs trial weighting, which is relatively complicated and time-wasting. As for the methods based on active control that zero-displacement and zero-force algorithms, high control performance is required to realize accurate unbalance calculation, which is however hard to achieve. Besides, introduction of notch filter or other methods to realize zero-displacement or zero-force control will change the closed-loop transfer function of the original control system, so it will bring about stability problems.

This paper deals with a novel field dynamic balancing method for a rigid rotor shaft supported by AMB, which is a no-trial weight method without stability problems, because the observer and filter are introduced in open-loop mode. Furthermore, with band-pass filter extracting the fundamental frequency signal and compensation based on the frequency response measurement, unbalance identification accuracy will be effectively enhanced.

II. DYNAMICS MODELING OF THE ROTOR-AMB SYSTEM

A. System Description

The rotor shaft considered here has 5 degrees of freedom (DOF) suspension support by AMB, the schematic diagram of which is shown in Fig. 1. The two turbine disks are assembled at the two outer ends, which are balancing planes as well. The rotor shaft is driven by a surface-mounted permanent-magnet synchronous machine (SPMSM) in the middle.

The rotor shaft owns a relatively symmetric supporting

structure with a 3-DOF AMB at each end. The inertial coordinate system (X-Y-Z) is established at the mass center S of the rotor shaft. The linear and angular displacements of translational and tilt motions in radial directions are denoted by x_s, y_s, α_s and β_s. The rotary motion about the Z-axis is controlled by the SPMSM, the spinning speed of which is denoted by Ω. As shown in Fig. 1, the spans of the two AMB to mass center are a_1 and b_1 respectively. Similarly, the spans of the two displacement sensor sets to mass center are a_2 and b_2, and of balancing planes are a_3 and b_3 respectively.

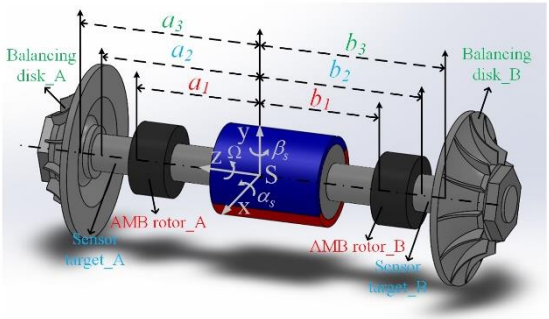

Fig. 1 The schematic diagram of the suspended rotor shaft

B. Dynamics of the Rotor Shaft

According to Newton's second law, the dynamical model of the rotor shaft with AMB can be presented as

$$\boldsymbol{M}\ddot{\boldsymbol{q}}_s + \boldsymbol{G}\dot{\boldsymbol{q}}_s = \boldsymbol{B}\boldsymbol{u} \tag{1}$$

where

$$\boldsymbol{M} = diag\left(I_{y0}, m, I_{x0}, m\right)$$

$$\boldsymbol{q}_s = \begin{bmatrix}\beta_s & x_s & -\alpha_s & y_s\end{bmatrix}^T$$

$$\boldsymbol{G} = I_{z0}\Omega\begin{bmatrix}0 & 0 & 1 & 0\\ 0 & 0 & 0 & 0\\ -1 & 0 & 0 & 0\\ 0 & 0 & 0 & 0\end{bmatrix}$$

$$\boldsymbol{B} = \begin{bmatrix}a_1 & -b_1 & 0 & 0\\ 1 & 1 & 0 & 0\\ 0 & 0 & a_1 & -b_1\\ 0 & 0 & 1 & 1\end{bmatrix}$$

$$\boldsymbol{u} = \begin{bmatrix}f_{ax} & f_{bx} & f_{ay} & f_{by}\end{bmatrix}^T$$

Here, $\boldsymbol{q}_s$ denotes the state variable which forms the generalized coordinate of the principal inertia axis. m is the mass of the rotor shaft, and I_{x0}, I_{y0} and I_{z0} are moment of inertia of each axis respectively. $\boldsymbol{u}$ denotes the suspension forces of the two AMB in radial directions. $\boldsymbol{G}$ is called gyroscopic matrix in general, which represents gyroscopic effect.

C. Coordinate transformation relations

On account of misalignment of the principal inertia axis and geometric axis derived from mass unbalance, the relationship between the two coordinates can be expressed as

$$\boldsymbol{q}_s = \boldsymbol{q}_g + \boldsymbol{q}_0 \tag{2}$$

where $\boldsymbol{q}_g$ forms the generalized coordinates of geometric axis position, and $\boldsymbol{q}_0$ represents the misalignment, which can be described as

$$\boldsymbol{q}_0 = \begin{bmatrix}\sigma\cos\left(\Omega t+\gamma\right)\\ e\cos\left(\Omega t+\theta\right)\\ \sigma\sin\left(\Omega t+\gamma\right)\\ e\sin\left(\Omega t+\theta\right)\end{bmatrix} \tag{3}$$

where e and θ are amplitude and initial phase of the distance of $\boldsymbol{q}_g$ and $\boldsymbol{q}_s$, and σ, γ are of the inclination angle.

Then we define the coordinates of AMB rotor motion that $\boldsymbol{q}_x = \begin{bmatrix}x_{xa} & x_{xb} & y_{xa} & y_{xb}\end{bmatrix}^T$, which denote the displacement of two AMB rotors in X- and Y- directions. Similarly, the displacement measurement coordinates are defined that $\boldsymbol{q}_m = \begin{bmatrix}x_{ma} & x_{mb} & y_{ma} & y_{mb}\end{bmatrix}^T$, which denote the measured values picked up by eddy current sensors.

According to the geometrical relationship of the rotor-AMB system, the relationship of these coordinates can be expressed as

$$\boldsymbol{q}_x = \boldsymbol{T}_x\boldsymbol{q}_g,\ \ \boldsymbol{q}_m = \boldsymbol{T}_m\boldsymbol{q}_g \tag{4}$$

where $\boldsymbol{T}_x = \begin{bmatrix}a_1 & 1 & 0 & 0\\ -b_1 & 1 & 0 & 0\\ 0 & 0 & a_1 & 1\\ 0 & 0 & -b_1 & 1\end{bmatrix}$, $\boldsymbol{T}_m = \begin{bmatrix}a_2 & 1 & 0 & 0\\ -b_2 & 1 & 0 & 0\\ 0 & 0 & a_2 & 1\\ 0 & 0 & -b_2 & 1\end{bmatrix}$.

D. Modeling of the AMB Supporting Rotor Shaft

In general, the magnetic force can be linearized approximately near the operating point, that the displacement and control current values are both near zero. Consequently, linearized model of magnetic bearing forces can be expressed as

$$\boldsymbol{u} = \boldsymbol{k}_s\boldsymbol{q}_x + \boldsymbol{k}_i\boldsymbol{I} \tag{5}$$

where $\boldsymbol{k}_s = diag\left(k_{sax},\ k_{sbx},\ k_{say},\ k_{sby}\right)$ is the displacement stiffness matrix, and $\boldsymbol{k}_i = diag\left(k_{iax},\ k_{ibx},\ k_{iay},\ k_{iby}\right)$ is the current stiffness matrix, which are both inherent properties of AMB; $\boldsymbol{I} = \begin{bmatrix}i_{ax} & i_{bx} & i_{ay} & i_{by}\end{bmatrix}^T$ denotes the control current matrix of four radial DOF.

According to (1)-(5), equation of rotor shaft motion can be derived as

$$\boldsymbol{M}\ddot{\boldsymbol{q}}_g = -\boldsymbol{G}\dot{\boldsymbol{q}}_g + \boldsymbol{B}\boldsymbol{k}_s\boldsymbol{T}_x\boldsymbol{q}_g + \boldsymbol{B}\boldsymbol{k}_i\boldsymbol{I} + \Omega^2\boldsymbol{M}_1\boldsymbol{q}_0 \tag{6}$$

where $\boldsymbol{M}_1 = diag\left(I_{y0}-I_{z0}, m, I_{x0}-I_{z0}, m\right)$. The equation of motion is expressed base on the coordinates of geometric axis position, which are observable. The terms on the right-hand side of the equation (6) are forces and torques respectively derived from gyroscopic coupling, displacement stiffness, current stiffness and mass unbalance.

III. PRINCIPLE OF THE FIELD DYNAMIC BALANCING METHOD

The novel field dynamic balancing method is based on disturbance observation and error compensation under open-loop mode, the block diagram of which is shown in Fig. 2. Based on the original suspension control, the balancing algorithm is introduced into the system shown in the dashed box.

An ESO is adopted to realize disturbance observation, and the band-pass filter to pick up the unbalance information. Then the estimation error is compensated based on the frequency response characteristics of the observation module combining the observer and filter. At last, balancing information can be calculated easily.

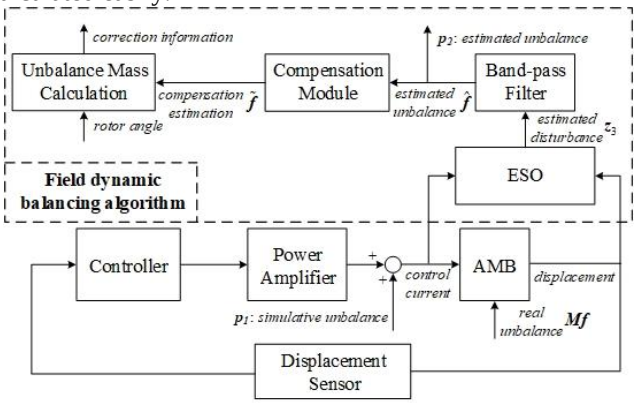

Fig. 2 Block diagram of field dynamic balancing based on ESO

A. Design of the ESO

Active disturbance rejection control (ADRC) was proposed to realize disturbance rejection [9], and ESO was the core technology, which can estimate all the disturbances on the plant in many application areas. Similarly, an ESO can be designed to estimate static and couple unbalances on the rotor shaft according to the equation of rotor shaft motion.

First of all, (6) is converted to an equation of motion state as

$$\begin{cases} \dot{\boldsymbol{q}}_1=\boldsymbol{q}_2 \\ \dot{\boldsymbol{q}}_2=-\boldsymbol{M}^{-1}\boldsymbol{G}\dot{\boldsymbol{q}}_1+\boldsymbol{M}^{-1}\boldsymbol{B}\boldsymbol{k}_s\boldsymbol{T}_x\boldsymbol{q}_1+\boldsymbol{M}^{-1}\boldsymbol{B}\boldsymbol{k}_i\boldsymbol{I}+\boldsymbol{q}_3 \\ \dot{\boldsymbol{q}}_3=\boldsymbol{g} \end{cases} \tag{7}$$

where $\boldsymbol{q}_1=\boldsymbol{q}_g$, $\boldsymbol{q}_3=\Omega^2\boldsymbol{M}^{-1}\boldsymbol{M}_1\boldsymbol{q}_0+\boldsymbol{d}$ and $\boldsymbol{g}=\begin{bmatrix} g_1 & g_2 & g_3 & g_4 \end{bmatrix}^T$. Here, a term $\boldsymbol{d}$ is added to denote other disturbs such as sensor runout disturbs or some other noises, which cannot be modeled accurately.

It is noted that gyroscopic effect can be neglected as for a slender rotor like the rotor shaft in this paper, as the term $\boldsymbol{M}^{-1}\boldsymbol{G}\dot{\boldsymbol{q}}_1$ in (7) is relatively small. Accordingly, ESO can be designed as

$$\begin{cases} \boldsymbol{e}_1=\boldsymbol{z}_1-\boldsymbol{q}_1 \\ \dot{\boldsymbol{z}}_1=\boldsymbol{z}_2-\beta_1\boldsymbol{e}_1 \\ \dot{\boldsymbol{z}}_2=\boldsymbol{z}_3-\beta_2\boldsymbol{e}_1+\boldsymbol{M}^{-1}\boldsymbol{B}\boldsymbol{k}_s\boldsymbol{T}_x\boldsymbol{q}_1+\boldsymbol{M}^{-1}\boldsymbol{B}\boldsymbol{k}_i\boldsymbol{I} \\ \dot{\boldsymbol{z}}_3=-\beta_3\boldsymbol{e}_1 \end{cases} \tag{8}$$

in which the parameter $\boldsymbol{z}_3=\begin{bmatrix} z_{31} & z_{32} & z_{33} & z_{34} \end{bmatrix}^T$ containing unknown disturbs is the estimated output, and β_1, β_2, β_3 are the parameters in ESO.

Neglecting the term $\boldsymbol{M}^{-1}\boldsymbol{G}\dot{\boldsymbol{q}}_1$ and subtracting (7) from (8), the error equation can be obtained as

$$\begin{cases} \dot{\boldsymbol{e}}_1=\boldsymbol{e}_2-\beta_1\boldsymbol{e}_1 \\ \dot{\boldsymbol{e}}_2=\boldsymbol{e}_3-\beta_2\boldsymbol{e}_1 \\ \dot{\boldsymbol{e}}_3=-\boldsymbol{g}-\beta_3\boldsymbol{e}_1 \end{cases} \tag{9}$$

where $\boldsymbol{e}_2=\boldsymbol{z}_2-\boldsymbol{q}_2$ and $\boldsymbol{e}_3=\boldsymbol{z}_3-\boldsymbol{q}_3$. And the stability of the error equation can be easily verified based on its characteristic equation when the parameters and control period are appropriate values. Thus each terms of (9) could approach zero, thus

$$\begin{cases} \boldsymbol{e}_1=-\beta_3^{-1}\boldsymbol{g} \\ \boldsymbol{e}_2=-\beta_1\beta_3^{-1}\boldsymbol{g} \\ \boldsymbol{e}_3=-\beta_2\beta_3^{-1}\boldsymbol{g} \end{cases} \tag{10}$$

which means when β_3 is big enough, $\boldsymbol{e}_1$, $\boldsymbol{e}_2$ and $\boldsymbol{e}_3$ will all approach zero. Then $\boldsymbol{z}_3\to\boldsymbol{q}_3=\Omega^2\boldsymbol{M}^{-1}\boldsymbol{M}_1\boldsymbol{q}_0+\boldsymbol{d}$ will be obtained. Consequently, the observation target existing in the misalignment value $\boldsymbol{q}_0$ can be picked up from $\boldsymbol{z}_3$ after convergence, and here we define the real unbalance information $\Omega^2\boldsymbol{M}^{-1}\boldsymbol{M}_1\boldsymbol{q}_0=\boldsymbol{f}=\begin{bmatrix} f_1 & f_2 & f_3 & f_4 \end{bmatrix}^T$.

According to Lyapunov criteria, if all the characteristic values of the characteristic polynomial are less than zero, the system will own Lyapunov stability. Besides, the form of a third order characteristic equation with good static and dynamic performance is $(s+k)^3$. Thus, the characteristic equation of (9) is usually selected as follows:

$$\begin{aligned} (s+k)^3 &= s^3+3ks^2+3k^2s+k^3 \\ &= s^3+\beta_1s^2+\beta_2s+\beta_3 \end{aligned} \tag{11}$$

Hence the three parameters can be expressed by one parameter.

B. Design of the Band-pass Filter

As mentioned above, the disturb observation mainly contains mass unbalances, sensor runout disturbs and some other noises. So extracting the mass unbalance information from $\boldsymbol{z}_3$ is worth thinking about, which is denoted by $\hat{\boldsymbol{f}}=\begin{bmatrix} \hat{f}_1 & \hat{f}_2 & \hat{f}_3 & \hat{f}_4 \end{bmatrix}^T$. Since the main characteristic of mass unbalance disturb is that the signal frequency is the same as that of rotor rotational speed rather than the multi-frequency disturbs derived from sensor runout or other noises. Therefore, removing useless signal $\boldsymbol{d}$ from $\boldsymbol{z}_3$ could be based on frequency domain features.

Switched capacitor filter has been widely used in measurement system of mechanical balancing machines, which is a band-pass filter to extract signals with certain frequency. The transfer function of this filter can be described as

$$H(s)=\frac{\frac{\omega_r}{Q}s}{s^2+\frac{\omega_r}{Q}s+\omega_r{}^2} \tag{12}$$

where Q is the quality factor, and ω_r is the band-pass center frequency, which could be set to be the rotational frequency. It can be easily derived from (12) that its bandwidth is

$$BW3dB=\frac{\omega_r}{Q} \tag{13}$$

which represents that with smaller center frequency or bigger quality factor, the bandwidth will be narrower, and it exactly meets the requirements of signal extraction. However, the rate of the filter convergence will be slower if the bandwidth is narrow, because of the bad attenuation ability for signals within stopband. Thus the value of Q need to be selected specially for tradeoff between the band-pass performance and rate of convergence.

Consequently, the above mentioned band-pass filter is cascaded after the ESO output with the passband frequency the same as that of rotational speed. Then the harmonic disturbs and other noises which are major factors affecting the unbalance identification precision will be eliminated. Above all, $\hat{\boldsymbol{f}}\rightarrow\boldsymbol{f}$ can be obtained through the observation module combined with ESO and band-pass filter.

C. Compensation of the Identified Unbalance

It is noted that the ESO and the band-pass filter both have their own frequency characteristics, not only in amplitude but also in phase values. Therefore, if unbalance mass was directly calculated by the estimated unbalance $\hat{\boldsymbol{f}}$, there would be estimation errors.

In order to enhance the identified accuracy, compensation for the observation error should be carried out. Based on the frequency characteristics of the observation module that the relationships between $\boldsymbol{f}$ and $\hat{\boldsymbol{f}}$ in varies frequencies, the estimation errors can be derived for compensation.

However, the real unbalance $\boldsymbol{f}$ is hard to be obtained, thus an equivalent measuring method can be carried out. When the rotor shaft is suspended in static state, through injecting simulated unbalance signals into control coil current, which are denoted by $\boldsymbol{p}_1$ in Fig. 2, the estimated unbalance will be obtained from the observation module as represented by $\boldsymbol{p}_2$. Subsequently, after comparing the signal $\boldsymbol{p}_1$ and $\boldsymbol{p}_2$, the response features in balancing frequency can be obtained. Furthermore, the frequency response characteristics can be derived through sweep frequency test, with which the unbalance disturbs could be identified accurately in full speed range.

After the frequency features being acquired off-line, the rotor shaft can be driven in balancing rotational speed, and accurate unbalance disturbs could be identified after observation and compensation on-line. In other words, $\tilde{\boldsymbol{f}}\approx\boldsymbol{f}$ can be obtained, where $\tilde{\boldsymbol{f}}$ denotes the observations after compensation.

D. Correction Mass Calculation

With the accuracy unbalance disturbs identified, correction mass can be calculated easily. Supposing that the correction masses are added on the balancing disks, the weights of which are m_a and m_b respectively, and the angles are δ_a and δ_b. Thus the relations of correction masses can be described as

$$\begin{cases} m_{ax}^2+m_{ay}^2=m_a^2 \\ \delta_{\mathrm{a}}=\arctan\left(\dfrac{m_{ay}}{m_{ax}}\right) \\ m_{bx}^2+m_{by}^2=m_b^2 \\ \delta_b=\arctan\left(\dfrac{m_{by}}{m_{bx}}\right) \end{cases} \tag{14}$$

where m_{ax} and m_{ay} denote the equivalent masses of balancing disk_A in X- and Y- direction respectively; m_{bx} and m_{by} denote that of balancing disk_B as well. Thus the correction forces and torques can be derived as

$$\boldsymbol{T}=\begin{bmatrix} a_3 & -b_3 & 0 & 0 \\ 1 & 1 & 0 & 0 \\ 0 & 0 & -a_3 & b_3 \\ 0 & 0 & 1 & 1 \end{bmatrix}\Omega^2\begin{bmatrix} m_{ax}r_a \\ m_{bx}r_b \\ m_{ay}r_a \\ m_{by}r_b \end{bmatrix} \tag{15}$$

where r_a and r_b are radius of the two balancing disks.

In order to balance the unbalance disturbs and the corrections, the relations should be maintained as

$$\Omega^2\boldsymbol{M}_1\boldsymbol{q}_0+\boldsymbol{T}=0 \tag{16}$$

Consequently, with the compensation observation $\tilde{\boldsymbol{f}}\approx\boldsymbol{f}=\Omega^2\boldsymbol{M}^{-1}\boldsymbol{M}_1\boldsymbol{q}_0$, the correction information contained in $\boldsymbol{T}$ can be derived based on (16).

IV. Simulation Analysis

In this section, computer simulations are performed to validate the effectiveness of the proposed dynamic balancing method. The simulation model is established based on a high-speed centrifugal compressor supported by AMB, as shown in Fig. 1.

A. Unbalance Observation

For a practical rotor shaft, it is difficult to ascertain the unbalance distribution in advance, so the simulation which is aimed to verify the unbalance observation effectiveness is performed by exerting known simulative unbalance on the rotor shaft. Thus the unbalance denoted by $\boldsymbol{q}_0$ is predefined, of which the amplitude and initial phase are set as e=30μm, θ=150°, σ=0.05° and γ=60°, and sensor runout disturbs are also simulated by third- and fifth harmonic signals.

The displacement orbits of the two AMB rotor are

illustrated in Fig. 3 where the rotor shaft speed is hold at 10,000 r/min (167Hz).

Subsequently, ESO and band-pass filter are activated, of which the parameters are adjusted as k=15000 , Q=10 , ω_r=167Hz . And then the outputs of the ESO with and without band-pass filter are obtained as shown in Fig. 4, where the figure (a) illustrates the unbalance disturbance toque about Y-axis, and the figure (b) illustrates the unbalance force in X-direction. With these two observation values, information to calculating correction mass is sufficient for the trigonometrical function relationship between $\hat{f}_1$, $\hat{f}_2$ and $\hat{f}_3$, $\hat{f}_4$.

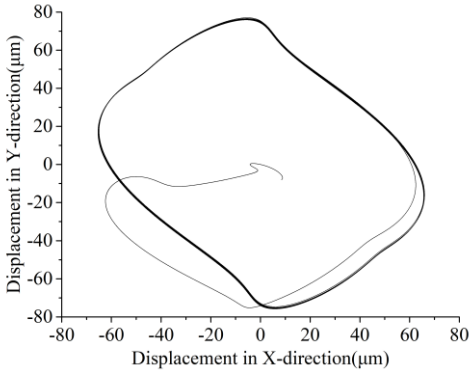

(a)

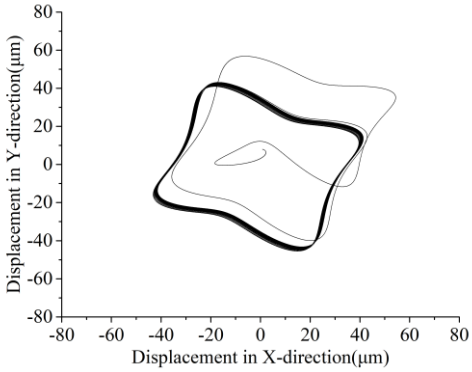

(b)

Fig. 3 Displacement orbits of the two AMB at 10000r/min.
(a)AMB_A; (b)AMB_B

The simulation results show that the effectiveness of the mass unbalance observation module combined with ESO and band-pass filter. Besides, even though the observation has come into stable state, the amplitude and phase of that still have observation errors. Thus the error compensation is of the essence, which will be elaborated in the next section.

B. Acquisition of Frequency Response Characteristics

On account of the observation error mentioned above, the frequency response characteristics of the observation module are measured for compensation. Through exerting known unbalance disturbs with varying frequencies into the rotor-AMB system and comparing with the outputs of the observation module, the frequency response can be obtained easily, which of $\hat{F}_1(s)/F_1(s)$ is illustrated in Fig. 5 as an example.

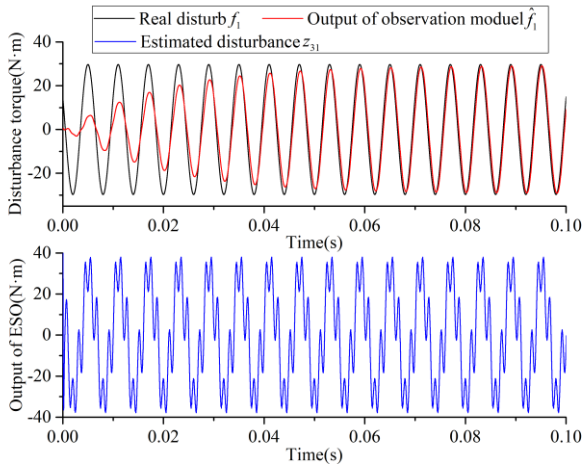

(a)

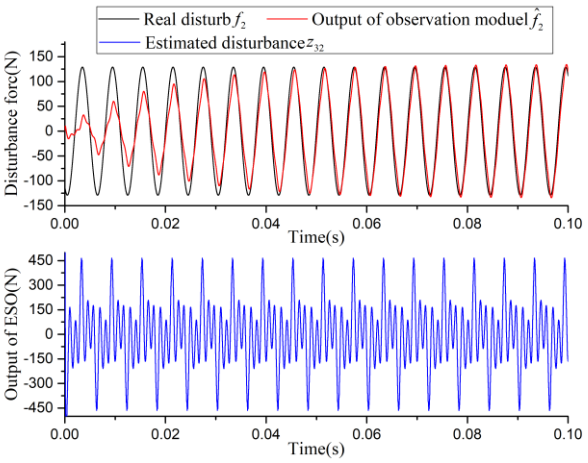

(b)

Fig. 4 Disturb observation results.
(a)Disturbance torque about Y-axis; (b)Disturbance force in X-direction.

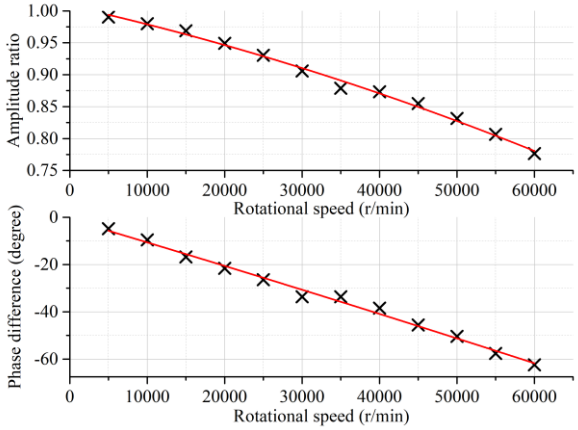

Fig. 5 Frequency response characteristics of observation module

In Fig. 5, curves are drawn to fit the discrete sample datum, which is to show the characteristic variation tendency with rotational speed increasing. As we can see, when rotor shaft rotates faster, the observation errors become larger not only in amplitude estimations but also in phase estimations. In actual compensation process, the frequency response characteristic datum at balancing rotational speed will be employed.

Based on the features at the mimic balancing speed (10000r/min), that the amplitude ratio and phase difference of f_1 to $\hat{f}_1$ are obtained to be 0.98 and 9.6° respectively, and those of f_2 to $\hat{f}_2$ be 0.966 and 12° respectively. Besides, the amplitude and phase of $\hat{f}_1$ are 29.1N·m and 50.4° respectively, and those of $\hat{f}_2$ are 124.54N and 139.2° respectively.

Above all, the amplitude and phase of real unbalance $\tilde{f}_1$ are $29.7\mathrm{N}\cdot\mathrm{m}$ and $60°$ respectively, and those of $\tilde{f}_2$ are 128.93N and $151.2°$ respectively. Comparing with the simulated predefined unbalance as

$$f_1=\Omega^2\left(I_{y0}-I_{z0}\right)\sigma\cos\left(\Omega t+\gamma\right)=29.8\left(\Omega t+60^\circ\right)\mathrm{N}\cdot\mathrm{m}$$
$$f_2=\Omega^2 me\cos\left(\Omega t+\theta\right)=129.5\cos\left(\Omega t+150^\circ\right)\mathrm{N} \quad (17)$$

Thus we can conclude that the unbalance observation after compensation is accurate reasonably.

V. CONCLUSION

A novel field dynamic balancing method for rigid rotor shafts is proposed based on AMB controllers. In this method, an extended state observer and a filter are designed to identify the unbalance disturbances. The observation module is introduced in open-loop mode, which will not bring about stability problems. Subsequently, the identification errors are compensated based on frequency characteristics of the observation module. Through simulation results, we can find the algorithm can identify the unbalance values accurately, which are used for unbalance mass calculation in rotor dynamic balancing.

In addition, the simulation results look perfect because of the ideal simulation conditions, thus experimental realization and verification are much imperative and the subsequent experimental results will be discussed in future articles.

REFERENCES

[1] Liu, C. and G. Liu, "Field dynamic balancing for rigid rotor-AMB system in a magnetically suspended flywheel," *IEEE/ASME Transactions on Mechatronics*, 2015: p. 1-1.

[2] Bai Jinggang, Zhao lei, "Zhang Xiaozhang, Study on On-line Balance for AMB Rotors," *The First Chinese Symposium on Magnetic Bearings*, 2005.

[3] Hou Eryong, Liu Kun, "Parameter Identification for Magnetic Bearing Based on Online Dynamic Balancing," *Journal of National University of Defense Technology*, 2013: p. 65-70.

[4] Wei Beiping, "Study on Field Dynamic Balancing for Magnetic Bearing Rotor," *Nanjing University of Aeronautics and Astronautics*, 2009.

[5] Kai, Z. and X. Zhang, "Rotor Dynamic Balance Making Use of Adaptive Unbalance Control of Active Magnetic Bearings," *in Intelligent System Design and Engineering Application (ISDEA), 2010 International Conference on*. 2010. p. 347-350.

[6] Xu, X. and S. Chen, "Field Balancing and Harmonic Vibration Suppression in Rigid AMB-Rotor Systems with Rotor Imbalances and Sensor Runout," *Sensors*, 2015. 15(9): p. 21876-21897.

[7] Pu Pengcheng, Zhang Kai, Yu Jinpeng, Zhao Lei, "On-line Balancing of High-speed Magnetic Suspended Flywheel System under Force Free Control of Imbalance," *Optics and Precision Engineering*, 2017(07): p.1796-1806.

[8] Fang, J., et al., "Field Balancing of Magnetically Levitated Rotors without Trial Weights," *Sensors*, 2013. 13(12): p. 16000-16022.

[9] Han, J., "Auto-disturbances-rejection Controller and Its Applications," *Control & Decision*, 1998.